Journal of Sol-Gel Science and Technology 36, 285–292, 2005

DOI: 10.1007/s10971-005-4662-1

Hydrophobic and Physical Properties of the Two Step Processed Ambient Pressure Dried Silica Aerogels with Various Exchanging Solvents

A. PARVATHY RAO* AND A. VENKATESWARA RAO
Airglass Laboratory, Physics Department, Shivaji University, Kolhapur-416004, Maharashtra, India
parvathy_shivaj@yahoo.co.in
avrao_phy@unishivaji.ac.in

G.M. PAJONK
Laboratoire Des Materiaux et Procedes catalytiques, Universite Claude Bernard, Lyon1,43 Boulevard Du11Novembre 1918, 69622 Villeurbanne Cedex, France

Received July 7, 2005; Accepted August 30, 2005

Abstract. The experimental results by using various exchanging solvents in the preparation of two step (acid and base) processed ambient pressure dried hydrophobic silica aerogels, are reported. Silica alcogels were prepared by hydrolysis with oxalic acid and condensation with NH_4OH of ethanol diluted tetraethylorthosilicate (TEOS) precursor and hexamethyldisilazane(HMDZ) methylating agent. The exchanging solvents used were: hexane, cyclohexane, heptane, benzene, toluene and xylene. The physical properties such as % of volume shrinkage, density, pore volume, % of porosity, thermal conductivity, % of optical transmission, surface area, pore size distribution and contact angle (θ) of the silica aerogels with water, were measured as a function of EtOH/TEOS molar ratios (R) for all the exchanging solvents. It was found that the physical and hydrophobic properties of the silica aerogels strongly depend on the nature of the solvent and R. Heptane solvent resulted in highly transparent (≈90% optical transmission at 700 nm for 1 cm thick sample), low density (≈0.060 g/cm^3), low thermal conductive (≈0.070 W/m·K), high % of porosity (97%), high surface area (750 m^2/g), uniform porosity and hydrophobic ($\theta \approx 160^\circ$) aerogels compared to other solvents. On the otherhand, xylene resulted in aerogels with higher hydrophobicity ($\theta \approx 172^\circ$) among other solvents.

Key words: microporous, sol-gel chemistry, hydrophobicity, thermal conductivity, optical transmission

1. Introduction

Aerogels are among the most versatile materials available for technological and scientific applications because of their exceptional properties particularly homogeneity and uniformity, low density (0.05–0.30 g/cm^3), high porosity (≈95%) high surface area (500–1200 m^2/g), low dielectric constant (≈1.5) and low thermal conductivity (≈0.01–0.15 W/mK) [1, 2]. They are used in laser experiments, sensors, nuclear particle detectors, waste management (gas absorption, radioactive waste confinement) optics and light guides, MOSFETs, capacitors, energy storage, high explosive research, imaging devices catalysts and X-ray laser research [3–7]. Generally, silica aerogels are produced using supercritical drying method as originally done by Kistler [8]. However, this is an expensive and risky method because of the high pressures (8–10 MPa) and high temperatures (250–270°C) are involved. The shrinkage in the alcogels is largely irreversible, as the pore surfaces come together, silanol groups on the surface condense and lock the structure in the collapsed

*To whom correspondence should be addressed.

state. This irreversibility of the shrinkage is prevented by end capping of the silanols, so that after the solvent has been evaporated, deformation is elastic as reported in earlier publications [9–14]. The end capping is done by the attachment of the trimethylsilyl groups to the end groups (Si–OHs) of the pore surfaces. The present paper reports the research results on the preparation and physical properties of the ambient pressure dried silica aerogels using tetraethylorthosilicate (TEOS) and two step acid and base catalysed process with EtOH/TEOS molar ratio (R) variation from 4 to 16 and hexamethyldisilazane (HMDZ) surface modification by varying the exchanging solvents such as hexane, cyclohexane, heptane, benzene, toluene and xylene.

2. Experimental

Hydrophobic silica aerogels were prepared by two step acid base sol-gel process followed by ambient pressure drying using tetraethylorthosilicate [TEOS] precursor, oxalic acid [$C_2H_2O_4$, $2H_2O$, OXA] and ammonium hydroxide [NH_4OH] catalysts and HMDZ methylating agent. The preparation method is clearly explained in our previous paper [15]. Figure 1 shows the flow chart of the preparation of the hydrophobic silica aerogels by ambient pressure drying method. The silica alcosols were prepared by keeping the molar ratio of TEOS:acidic H_2O:basic H_2O:OXA:NH_4OH:HMDZ constant at 1:3.75:2.25:6.23 $\times$ 10^{-5}:4 $\times$ 10^{-2}:0.36 respectively and varying the R from 4 to 16. In the first step, to the ethanolic TEOS, water with oxalic acid was added and stirred thoroughly and kept in 50 ml beakers at room temperature for 24 h for hydrolysis. Then water with ammonium hydroxide was added and stirred and kept at room temperature for gelation.The gels were put in the oven at 50°C for 3 h for strengthening. The solvent in the gels was exchanged with each exchanging solvent three times in 48 h. Then the gels were immersed in 5% HMDZ in the solvent for 24 h. Unreacted HMDZ was exchanged with the solvent two times in 36 h. Finally the solvent was decanted and the gels were put in the oven at 50°C for 6 h, 150°C for 24 h and 200°C for 12 h. The resulting aerogels were cooled to room temperature and the physical properties of the aerogels were studied.

3. Characterization

The % of volume shrinkage, density, pore volume, % of optical transmission, % of porosity, thermal conductivity and contact angle of the silica aerogels were measured. The density was measured by measuring the weight and volume of the aerogels. Weight was measured with a microbalance of 10^{-5} g precision. The % of volume shrinkage and % of porosity were calculated using the following equations:

$$\%\ \text{of volume shrinkage} = \left(1 - V_a/V_g\right) \times 100 \qquad (1)$$

$$\%\ \text{of porosity} = \left(1 - \rho_b/\rho_s\right) \times 100 \qquad (2)$$

where V_a and V_g are the volumes of the aerogel and alcogel respectively, ρ_b and ρ_s are the bulk and sketetal densities of the silica aerogel respectively.

The thermal conductivity was measured using thermal ring probe sandwitched in between two identical aerogel samples [C-T meter from Teleph Company, France]. The sensitivity of the C-T meter is 0.001 W/mK. The contact angle of silica aerogels with water was measured using the Tantec contact angle meter, USA. The % of optical transmission was measured using Systronic 119 optical spectrophotometer at 700 nm. Fourier Transform Infrared spectroscopic (FTIR) studies were carried out using Perkin Elmer

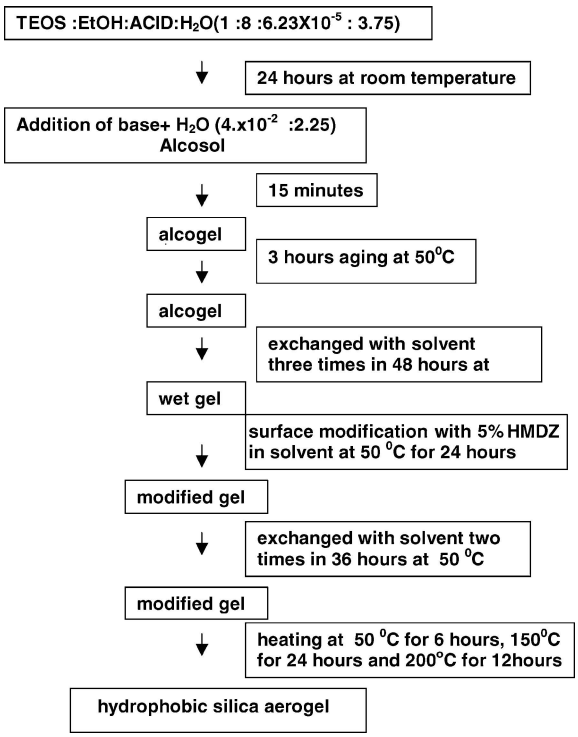

Figure 1. Flow diagram of the preparation of ambient pressure dried hydrophobic silica aerogels.

Table 1. Some of the Physical constants of the solvents used in the work [16].

Name	Formula	Molecular weight	Viscosity (mp)	Vapour pressure at 30°C (mm/Hg)	Surface tension 10^{-7} Nm^{-1}
Water	H_2O	18	10.087	–	72.75
Methanol	CH_3OH	32	5.93	160	22.60
Ethanol	C_2H_5OH	47	11.943	78.8	22.75
Hexane	C_6H_{14}	86	3.26	188.6	18.40
Cyclohexane	C_6H_{12}	84	9.3	121.3	25.30
Heptane	C_7H_{16}	100	4.163	58.35	19.65
Benzene	C_6H_6	78.11	6.47	118.24	29.02
Toluene	C_6H_5 CH_3	92	5.903	36.27	28.50
Xylene	C_6H_4 $(CH_3)_2$	106.17	8.102	16.35	28.37

(Model no. 760x in 450–4000 cm^{-1} range) IR spectrophotometer.

Surface area was determined via five point BET analysis from the amount of N_2 gas adsorbed at various partial pressures ($0.05 < p/p_0 < 0.3$, nitrogen molecular cross-sectional area = 16.2 $Å^2$).

The pore size distributions were measured via nitrogen desorption isotherms, using as ASAP 2000 by Micromeritics. A single condensation point ($p/p_0 = 0.99$) was used to find the pore radius (r) using the Kelvin equation:

$$\ln(p/p_o) = -2\gamma V/rRT \qquad (3)$$

This equation establishes a relationship between pore radius (r) and the relative pressure (p/p_0) employed in the N_2 adsorption–desorption technique. The symbols V and r represent the molar volume and the surface tension of the condensed liquid (N_2) in the pores. The pore volume was calculated by using the relation:

$$\text{pore volume} = (1/\rho_b - 1/\rho_s)\ \text{cm}^3/\text{g} \qquad (4)$$

4. Results and Discussion

The physical properties of the aerogels strongly depend on the nature of the exchanging solvent. Some of the physical properties of the exchanging solvents are given in Table 1 [16]. The change in the % of volume shrinkage, pore volume and contact angle of the aerogels with the variation of the R from 4 to 16 for various solvents are given in Table 2. Figures 2 and 3 show the change in the density and the % of porosity of the aerogels with the variation of the R for various solvents. It is seen from Table 2 and Figs. 2 and 3, that the % of volume shrinkage and density, with various solvents is in the increasing order of heptane < xylene < hexane < toluene < cyclohexane < benzene and whereas pore volume and % of porosity is in the decreasing order of heptane > xylene > hexane > toluene > cyclohexane > benzene.

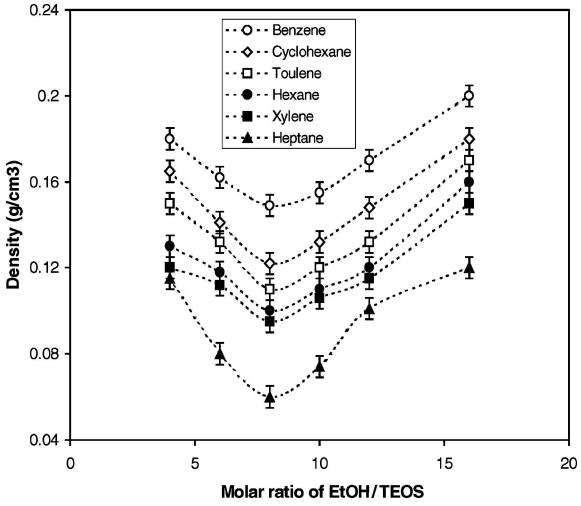

Figure 2. Change in the density of the silica aerogels with the variation of the EtOH/TEOS molar ratio (R) for various exchanging solvents.

The shrinkage of a gel during drying due to the capillary pressure P_c of the pore solvent is given by

Table 2. Physical and hydrophobic properties of the ambient pressure dried silica aerogels.

EtOH/TEOS	Benzene	Cyclohexane	Toluene	Hexane	Xylene	Heptane
			% of volume shrinkage $(V_g - V_a)/V_g \times 100$			
4	48	35	25	20	18	16
6	28	25	18	12	10	7
8	20	15	12	8	5	4
10	30	24	15	13	11	9
12	37	35	25	22	17	15
16	50	45	42	40	35	32
			Pore Volume $(1/\rho_b - 1/\rho_s)$ $\rho_s = 1.9$ g/cm^3			
4	5.03	5.53	6.14	7.17	7.8	8.17
6	5.79	5.8	7.8	8.56	8.7	15.1
8	6.32	7.67	8.56	9.47	10	16.14
10	5.62	6.05	7.9	8.25	9.1	14.92
12	5.36	6.72	7.05	7.8	8.17	9.37
16	5.03	5.06	5.36	5.7	6.14	7.81
			Contact angle (θ)			
4	133	133	135	130	137	138
6	149	150	153	156	165	158
8	157	159	158	157	172	160
10	155	156	157	154	169	156
12	153	155	154	152	163	154
16	147	139	149	136	152	144

[17, 18],

$$P_c = 2\Upsilon_{LV}/(r_p - t) \tag{4}$$

assuming that the contact angle of the pore liquid with pore walls is zero [19]. Υ_{LV}, is surface tension of the pore liquid and r_p, is the pore radius and t, is the thickness of the surface absorbed layer. The capillary pressure can be reduced only by reducing the surface tension of the pore liquid or preparing the gel with a large pore size [9]. By drying the gels at an ambient pressure, surface tension between liquid and vapour cannot be avoided and shrinkage occurs until the capillary pressure is resisted by bulk modulus (*K*o) of the gel (i.e. modulus of the drained gel network) [20]. However, reversible shrinkage in the gels can occurr i.e., spring back, during the last stage of the drying, if the inner surface of the wet gel has been modified by silylation to hinder siloxane bond formation during drying [10, 21]. It was found that the drying of the gels in various pore solvents permit the decrease of capillary pressure by using the solvent with low surface tension. The gel network will not experience shrinkage as long as the capillary pressure is lower than or equal to the pristine

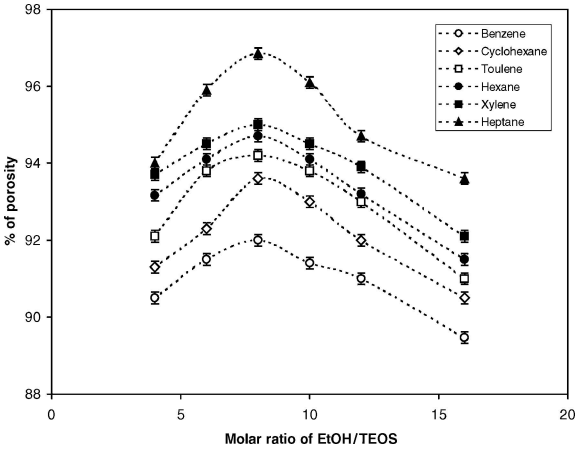

Figure 3. Change in the % of porosity of the silica aerogels with the variation of the EtOH/TEOS molar ratio (*R*) for various exchanging solvents.

gel strength. Supporting this conclusion, the solvents: heptane and xylene with low surface tension (even-though hexane has less surface tension than heptane, molecular weight and chain length of heptane play an

important role) produce less capillary pressure and the low vapour pressures of heptane and xylene cause less shrinkage in the gels during drying, therefore low density aerogels with less shrinkage were obtained.

Two phenomena which explain the solvent effects on silica alcogels are (1) variation of silica solubility and (2) structural modification. According to Kitahara et al. [22, 23] silica solubility decreases with increase of the solvent molecular weight. This effect causes variation in the shrinkage of the aerogels for different solvents [24]. The bulk density of the aerogels decreased for solvents of large chains. The contact angle between the pore walls and liquid decreased with molecular weight of the solvent [25], and has been found that the contact angle for these solvents was zero and capillary pressure depended only on the surface tension of the pore liquid and pore size of the silica network.Therefore it is suggested that the structural modification of the network by high molecular weight and long chain length solvents, is responsible for decreasing the density, high percentage of porosity and pore volume in the silica aerogels.

Dissolution and reprecipitation of silica gives coarsening because of the silica solubility and it is dependent on the primary particle/neck curvature. Silica is dissolved on the primary particle surface and redeposited around the point of contact to minimize the negative radius of the curvature (Oswald ripening). The rate of dissolution and reprecipitation of silica is also influenced by the type of pore solvent [26].

With the increase of R from 4 to 16, the percentage of shrinkage and density of the aerogels decreased, whereas the pore volume and percentage of porosity increased for R of 8 and percentage of shrinkage and density increased and pore volume and percentage of porosity decreased for further increase of $R >$ 8 as shown in Figs. 2 and 3 and Table 2. At lower R, due to insufficient EtOH, the availability of the free TEOS molecules is low, therefore the hydrolysis did not occur completely so the condensation occurred between hydrolysed and unhydrolysed species, therefore more shrinkage during drying leading to dense gels. At higher R (>8) due to the presence of excess ethanol [27], due to dilution, the distance between TEOS hydrolysed species is more, therefore continuous silica network did not form and hence during drying the gels shrink more resulting in dense gels. Low density aerogels have been obtained for R of 8 for various solvents.

The thermal conductivity of the aerogels decreased with increase of R to 8 and then increased with increase

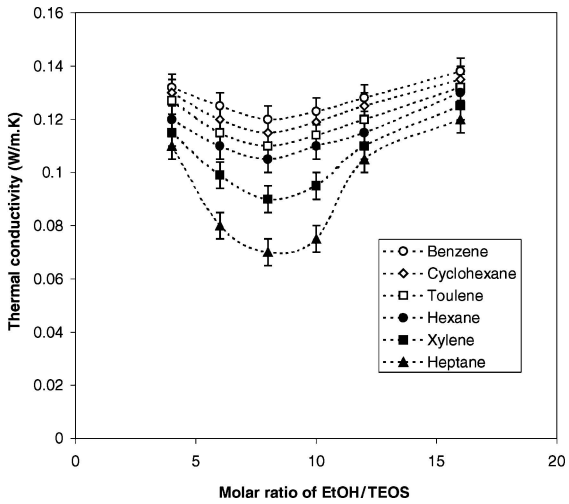

Figure 4. Change in the thermal conductivity of the silica aerogels with the variation of the EtOH/TEOS molar ratio(R) for various exchanging solvents.

of $R > 8$ for various solvents as shown in Fig. 4. The increasing order of thermal conductivity of the aerogels for various solvents is heptane $<$ xylene $<$ hexane $<$ toluene $<$ cyclohexane $<$ benzene. The thermal performance of the aerogels is strongly dependent on the particle, pore sizes and their distributions. The particle density or particle size is the first candidature to explain the trends in thermal conductivity. Change in the thermal conductivity results from the radiative and conductive heat transfer contributions and they effectively cancel each other out. This is due to the fact that the solid phase thermal conductivity is directly proportional while the radiative thermal conductivity is inversely proportional to the particle density [28]. The porosity dominates than particle volume in the silica aerogels hence to thermal conductivity is less. Among all the solvents, low thermal conductive aerogels (0.07 W/mK) are obtained with heptane because heptane produced with low density and high porosity the aerogels.

Figure 5 shows the percentage of optical transmission of the aerogels at 700 nm as a function of R from 4 to 16 for various solvents . It was found from the figure that the order of the percentage of optical transmission for various solvents at R of 8 is hexane $>$ cyclohexane $>$ heptane $>$ benzene $>$ xylene $>$ toluene. The optical transmission of the aerogels is largely a function of the particle size, size distribution, shape and particle density and surface roughness [29]. Optical clarity is governed by the light scattering resulting from

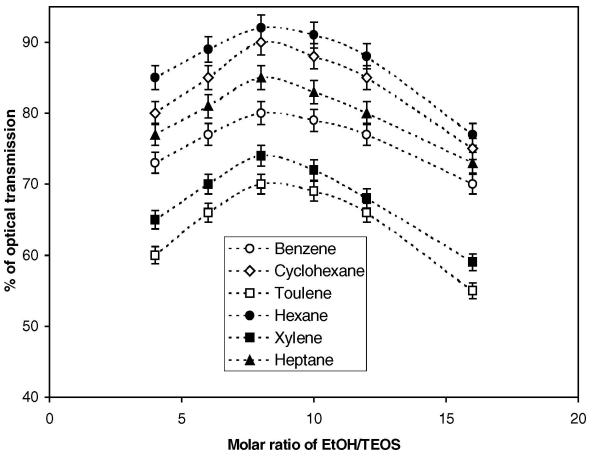

Figure 5. Change in the % of optical transmission of the silica aerogels with the variation of the EtOH/TEOS molar ratio (R) for various exchanging solvents at 700 nm.

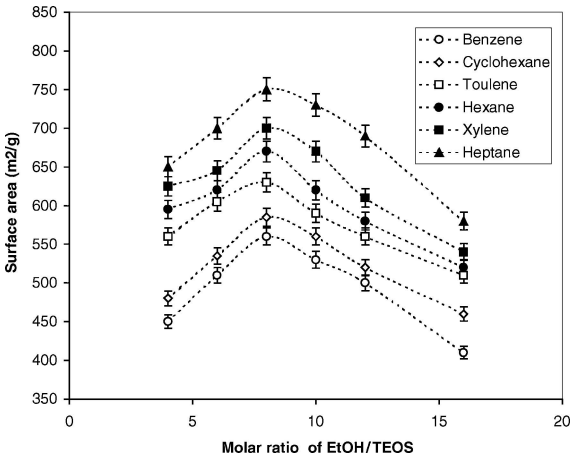

Figure 6. Change in the surface area of the silica aerogels with the variation of the EtOH/TEOS molar ratio (R) for various solvents.

inhomogeneities between the air and the solid matrix of the aerogels on small length scale in the nanometer range. In addition, scattering can result from the large macroscopic particles with inherent irregularities and surface roughness. The former is manupulated by the species from the sol–gel route to the network of the aerogel. The solvent is one of the primary factors to form the particles and the pore sizes because the pore size and particle size formation is dependent on the nature of the solvent. With toluene, bigger particle and pore sizes are formed and scattering is more with these aerogels hence the percentage of optical transmission is low where as hexane and cyclohexane produce smaller particle and pore sizes and therefore the aerogels with hexane and cyclohexane are more transparent. Hence, the type of solvent plays an important role in the production of transparent aerogels.

The change in the surface area of the aerogels with the variation of the R from 4 to 16 for various solvents is shown in Fig. 6. The order of the surface area for various solvents is benzene < cyclohexane < toluene < hexane < xylene < heptane. Low surface area silica aerogels were obtained with benzene because of more percentage of volume shrinkage and also irregular pore distribution in the aerogels whereas high surface area silica aerogels were obtained with heptane because of less percentage of volume shrinkage in the aerogels due to uniform porosity. The surface area of the samples increased with the increase of R to 8 and then decreased for R of >8. Irregular pore and particle sizes and more percentage of volume shrinkage occured in the silica

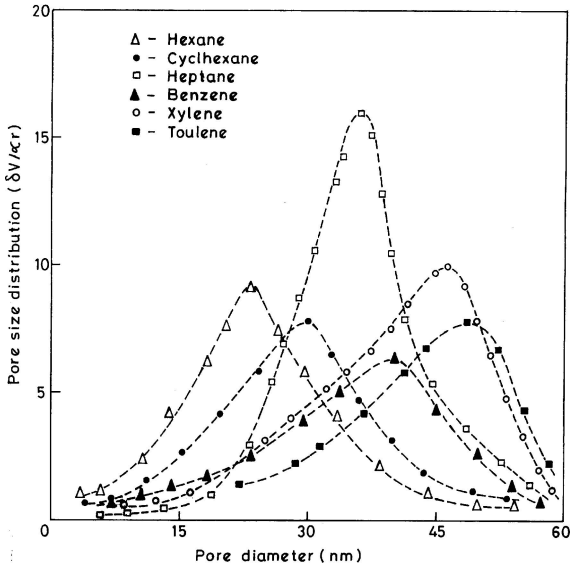

Figure 7. Pore size distributions of the silica aerogels for various solvents at EtOH/TEOS molar ratio (R) of 8.

aerogels for the R values of >8> therefore low surface area of the silica aerogels were obtained at the lower and higher of R at 8 .

Figure 7 shows the pore size distribution in the silica aerogels for various solvents at R of 8. The order of pore size distribution is hexane < cyclohexane < heptane < benzene < xylene < toluene. It was found from the figure that the silica aerogels obtained with hexane have small pore size distribution hence resulted in transparent silica aerogels where as in the case of toluene and xylene, bigger pore size distribution oc-

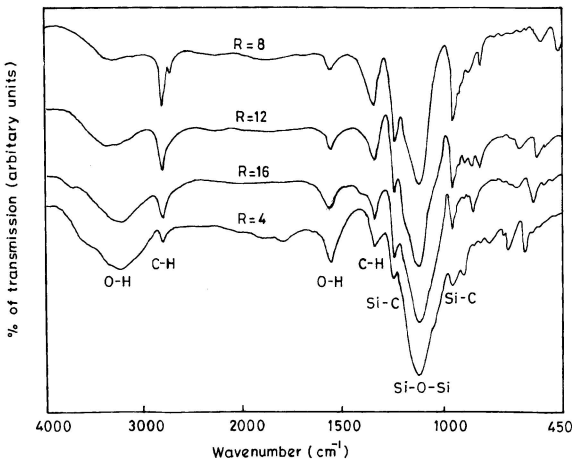

Figure 8. FTIR spectra of the silica aerogels with the variation of the EtOH/TEOS molar ratio (R).

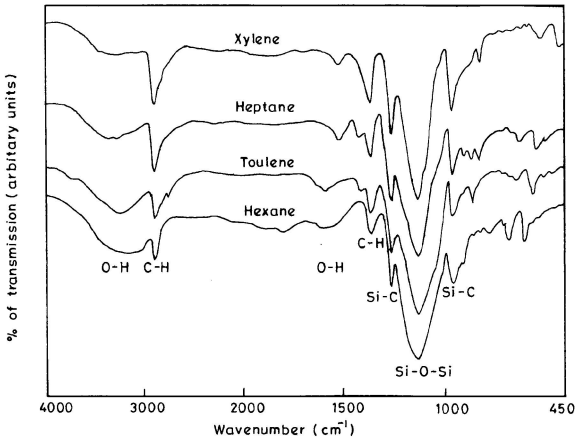

Figure 9. FTIR spectra of the silica aerogels for EtOH/TEOS molar ratio (R) of 8 for various solvents: (1) hexane (2) toluene (3) heptane (4) xylene.

curred and this led to transluscent silica aerogels. Uniform pore size distribution was observed in the silica aerogels with heptane therefore the resulting aerogels had less percentage of volume shrinkage and low density.

The hydrophobicity of the aerogels with various solvents has been observed as a function of R by measuring the contact angle (θ) of aerogels with water [30] and the results are shown in Table 2. It was found that for a solvent, the contact angle (θ) increased with the increase of R to 8 and then decreased for $R > 8$. Figure 8 shows the FTIR spectra of the silica aerogels with variation of the R for xylene solvent. It was observed that the intensity of the peaks at 840 and 1250 cm^{-1} of the Si–C and 2900 and 1450 cm^{-1} of the C–H [31, 32] increased with increase of R to 8 and decreased for R of >8. At R of <8<, the silica network is not uniform [33], leads to incomplete silylation of the surface of the silica network resulted, hence the intensities of the C–H and Si–H peaks were less. Therefore,the aerogels have low contact angle and hence are less hydrophobic. Figure 9 shows the FTIR spectra of the silica aerogels for various solvents for R of 8. It was observed that the intensities of peaks related to Si–H and C–H is more in the spectrum of xylene and similar intensities were obtained for other solvents. Therefore, all the solvents except xylene have similar contact angle values at R of 8. Xylene has the highest contact angle ($\approx$172°) because of its higher molecular weight and bigger size, it activates the silica surface for more silylation.

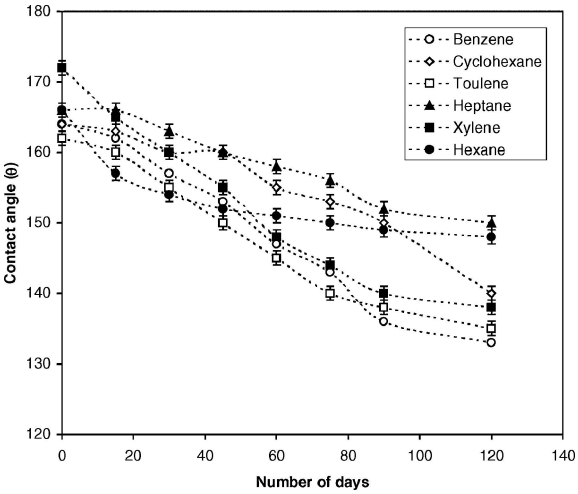

Figure 10. Change in the contact angle (θ) of the silica aerogels with time for various solvents.

Figure 10 shows the variation in the contact angle (θ) of the silica aerogels with time from 0 to 120 days. It was found that the decrease in the contact angle of the aerogels during 120 days with xylene solvent, is more (>30°) even though its initial contact angle is high and in the case of heptane, the decrease of the contact angle of the aerogels for 120 days is less ($\cong$10°).The atmospheric conditions have less effect on the heptane-based hydrophobic silica aerogels than xylene-based aerogels because of its physical properties. Low density, highly porous and hydrophobic, durable and low thermal conductive silica aerogels produced with the heptane solvent.

5. Conclusions

Ambient pressure dried hydrophobic silica aerogels were produced by using the tetraethylorthosilcate (TEOS) precursor with two step catalytic method and hexamethyldisilazane silylating (HMDZ) agent with various exchanging solvents. The solvents used were hexane, cyclohexane, heptane, benzene, toluene and xylene. The physical properties of the silica aerogels were measured with the variation of the EtOH/TEOS molar ratio (R) from 4 to 16 for these solvents. The % of shrinkage, % of porosity, density, porevolume, thermal conductivity, % of optical transmission, contact angle (hydrophobicity) of the silica aerogels with water were strongly dependent on the physical properties of the solvents such as surface tension, vapour pressure, molecular weight, chain length, viscosity. The hydrophobicity of the aerogels with the time from 0 to 120 days for these solvents has been studied and found that with the heptane solvent the decrease in the hydrophobicity of the silica aerogels was slow as compared to the other solvents. Low density (0.06 g/cm^3), highly porous (97%), hydrophobic ($\theta = 160^\circ$), low thermal conductive (0.07 W/mK) high surface area (750 m^2/g), uniform porosity and transparent (90%) silica aerogels were obtained with the heptane solvent and highly hydrophobic silica aerogels ($\theta = 172^\circ$), with xylene solvent.

Acknowledgments

The authors are highly thankful to the Department of Science and Technology (DST), New Delhi, for the funding this work under project No.SP/S2/CMP-01. One of the authors, A. Parvathy Rao is grateful to the DST for the Research Associateship.

References

1. L.W. Hrubesh, J. Non-Cryst. Solids **225**, 335 (1998).
2. C.A.M. Moulder and J.G. van Lierop, in *Aerogels*, edited by J. Fricke (Springer, Berlin, 1986), p. 68.
3. A.J. Hunt and K.D. Lofftus, Adv. Sol-Energy. Technol. **4**, 146 (1998).
4. V. Wittwer, J. Non-Cryst. Solids **145**, 233 (1992).
5. R. Gerlach, O. Kraus, J. Fricke, P.-Ch. Eccardt, N. Kroemer, and V. Magori, J. Non-Cryst. Solids **145**, 227 (1992).
6. G.M. Pajonk, App. Catal. **72**, 217 (1991).
7. G.M. Pajonk and S.J. Teichner, in *Aerogel*, edited by J. Fricke (Springer, Berlin, 1986), p. 193.
8. S.S. Kistler, Nature **27**, 741 (1931).
9. R. Deshpande, D.M. Smith, and C.J. Brinker, J. Non-Cryst. Solids **144**, 32 (1992).
10. S.S. Prakash, C.J. Brinker, A.J. Hurd, and S.M. Rao, Nature **374**, 439 (1995).
11. S.S. Prakash, C.J. Brinker, and A.J. Hurd, J. Non-Cryst. Solids **190**, 264 (1995).
12. H.S. Yang, S.Y. Choi, S.H. Hyun, H.H. Park, and J.K. Hong, J. Non-Cryst. Solids **221**, 151 (1997).
13. L. Duffours, T. Woignier, and J. Phalippou, J. Non-Cryst. Solids **186**, 321 (1995).
14. L. Duffours, T. Woignier, and J. Phalippou, J. Non-Cryst. Solids **194**, 283 (1996).
15. A. Parvathy Rao, G.M. Pajonk, and A. Venkateswara Rao, J. Mater. Sci. **40**, 1 (2005).
16. N.A. Lange (Ed.), *Handbook of Chemistry* (Handbook Publishers INC, Sandusky Ohio, 1946).
17. C.J. Brinker and G.W. Scherer, *Sol-Gel Science, The Physics and Chemistry of the Sol-Gel Processing* (Acedemic Press, San Diego, 1990).
18. G.W. Scherer, S. Haereid, E. Nilsen, and M.-A. Einarsrud, J. Non-Cryst. Solids **202**, 42 (1996).
19. D.J. Stein, A. Maskara, S. Haeireid, J. Anderson, and D.M. Smith, in *Better Ceramics Through Chemistry VI Mat. Res. Soc. Synthesis. Proc.* A.K. Cheetam, C.J. Brinker, M.A. Mc Cartney, and C. Sanchez (Eds.), (Pittsburg, PA 346 1994643).
20. D.M. Smith, G.W. Scherer, and J.M. Anderson, J. Non-Cryst. Solids **188**, 191 (1995).
21. D.M. Smith, D. Stein, J.M. Anderson, and W. Ackerman, J. Non-Cryst. Solids **186**, 104 (1995).
22. S. Kitahara, N. K. Zasski **90**, 237 (1969).
23. S. Kitahara, Chem. Abstr. **70**, 118461z (1969).
24. Mitsyuk Etal, B.M. Mitsyuk, Z.Z. Vysotski, and M.V. Polykov, Kokol Attad Nauk SSSR **155**(6), 416 (1964) (English version)
25. D.J. Stein, A. Maskara, S. Haeireid, J. Anderson, and D.M. Smith, in *Better Ceramics Through Chemistry VI Mater. Res. Soc. Proc.*, A.K. Cheetam, C.J. Brinker, M.A. Mc Cartney, and C. Sanchez (Eds.), Vol. 346.
26. R.K. Iler, *The Chemistry of Silica* (Wiley, New York, 1979).
27. B.E. Yoldas, J. Non-Cryst. Solids **63**, 145 (1984).
28. C.J. Brinker, US Patent 5,565,142.
29. W.C. Ackerman, M. Vlachos, R. Rouanet, and J. Fruendt, J. Non-Cryst. Solids **285**, 264 (2001).
30. F.A.L. Dullien, *Porous Media* (Academic Press, Sandiego, CA, 1991) p. 122.
31. C.J. Pouchert (Ed.), *Aldrich Library of FTIR Spectra* (Aldrich Chemical, Wisconsin, 1985) Vol. 2.
32. K. Lele, S.Y. Kim, and K.P. Yoo, J. Non-Cryst. Solids **186**, 18 (1995).
33. A. Venkateswara Rao, G.M. Pajonk, N.N. Parvathy, and E.E. Elaloui, in *Sol-gel Processing and Applications*, edited by A. Attia (Plenum Press, New York, 1994) p. 237.